IEICE Proceeding Series

A methodology for detecting and exploring non-convulsive seizures in patients with acute brain injury

DJ Albers, J Claassen, M Schmidt, G Hripcsak

Vol. 2 pp. 396-399
Publication Date: 2014/03/18
Online ISSN: 2188-5079

2013 International Symposium on Nonlinear Theory and its Applications
NOLTA2013, Santa Fe, USA, September 8-11, 2013

A methodology for detecting and exploring non-convulsive seizures in patients with acute brain injury

DJAlbers[†] and *JClaassen*[‡]and *MSchmidt*[‡] and *GHripcsak*[†]

†Department of Biomedical Informatics, Columbia University
622 West 168th Street VC-5, New York, NY, 10032, USA
‡Department of Neurology, Columbia University
710 West 168th Street, New York, NY, 10032, USA
Email: david.albers@dbmi.columbia.edu, jc1439@mail.cumc.columbia.edu, mjs2134@mail.cumc.columbia.edu, hripcsak@columbia.edu

Abstract—A methodology for detecting, identifying, and defining nonconvulsive seizures in individuals with acute brain injury is introduced. Specifically, beginning with an EEG signal, the power spectrum is estimated yielding a multivariate time series which is then analyzed using empirical orthogonal functional analysis. This methodology allows for identification and observation of seizures that are otherwise only identifiable though expert analysis of the raw EEG.

1. Introduction

Seizure detection in EEG data has a long history [8, 2, 6]. In fact, seizure detection has developed such that many clinically deployed EEG recording devices have proprietary seizure detection algorithms included. Nevertheless, automated seizure detection is not particularly effective. Moreover, most seizure detection is carried out in the context of epilepsy. Here we develop a methodology for identifying, detecting, and typify seizure in a different context, nonconvulsive seizures (NCSz) in *comatose* patients with a aneurysmal subarachnoid hemorrhage (SAH). The context is special for two reasons. First, SAH is a debilitating condition that affects a broad population. Second seizures in individuals with SAH are not well understood, may be diverse in type, and may affect recovery in different ways. Because of the potential diversity in seizure in SAH patients, we aim to both detect seizure events and discover and define different seizure types. Broadly, our methodology is based applying sequential targeted levels of analysis to raw data. More specifically, we estimate a power spectrum from EEG data on a moving window and then applying empirical orthogonal functional analysis (EOF) to the power spectrum (PS).

2. Seizures in individuals with SAH

Aneurysmal subarachnoid hemorrhage (SAH) occurs when blood enters the subarachnoid space, located between the arachnoid membrane and the pia mater surrounding the brain, from a ruptured dilated cerebral blood vessel. SAH affects up to 30,000 Americans annually carrying a huge public health burden. Secondary complications such as nonconvulsive seizures (NCSz) contribute significantly to poor outcome [1]. These seizures are different from convulsive seizures as the patients have no or minimal symptoms other than decreased mental status while the brain is seizing, making detection impossible in comatose patients. There is a great deal of evidence that suggests that additional brain injury occurs secondary to NCSz [1].

Treatment is available but diagnosis poses major challenges because SAH patients are usually comatose thus requiring detection from EEG alone and automated detection algorithms to date have very poor accuracy even for more well know seizure types. Controversy exists regarding the preferred treatment regimen but unanimously experts agree that the time to initiate treatment—soon after the onset of seizures—is much more important than the choice of seizure medication. Nevertheless, identification of the onset can be difficult and automated detection algorithms fall short as surface EEG is notoriously contaminated by artifact, including poor contact between EEG electrodes and scalp, sweat artifact, electrical artifact, etc. To combat some of these artifacts, intracrotical depth electrodes are increasingly placed together with other invasive brain monitoring devices and have the huge advantage of a better signal to noise ratio and better interpretation of other physiologic data collected invasively. Signals from such sources would be an ideal to further develop seizure detection algorithms with better specificity and sensitivity for seizures.

Diversity among seizures Seizures after acute brain injury show a great deal of phenotypical variability. For example, approximately half of the seizures remain focal and do not spread to other brain regions. Patterns of seizures further differ greatly in terms of maximum frequency, amplitude, duration, and background in between discharges. The pathophysiological significance of these differences is unknown but to study these differences accurate characterization of patterns is the first step.

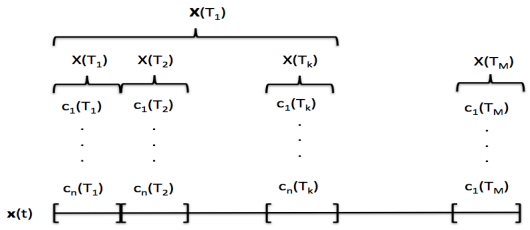

Figure 1: Broad view of our seizure analysis methodology. Given a time series ($\mathbf{x}(t)$), we estimate a power spectra at fixed intervals yielding powers per frequency ($c_i(T_j)$) that are then treated as a multi-variate time series ($\mathbf{X}(T_i)$) that is then studied using EOF analysis.

3. Seizure detection and analysis

General decomposition of a time series Begin with a time series of length MT, $\mathbf{x}(MT) = (x(1), x(2), \cdots, x(MT))$; the time series $\mathbf{x}(MT)$ can be split into M components indexed by k and denoted by $\mathbf{x}_k(t)$. Assume over the time period or window of calculation that the time series is ergodic and obeys the weak stationarity property [3, 7]. In this paper we will begin with an already estimated power spectrum of the EEG on a moving window forming at a time series of finite length, MT. We split this time series into M components of length T and then decompose the disjoint time series on the M windows using an EOF analysis.

Power spectra decomposition of EEG data One way to represent a time series is via a decomposition into a set of $2n$ frequencies [3], λ_j, or $\mathbf{x}_k(t) = \sum_{j=-n}^{n} c_j e^{i\lambda_j t}$; this representation of $\mathbf{x}_k(t)$ is called the Fourier transform [9, 3, 4] of $\mathbf{x}_k(t)$. In this framework $\mathbf{x}_k(t)$ is conceptualized as a collection of harmonic terms parameterized by frequency. Each frequency, λ_j, has an instantaneous power associated with it $|c_j|^2$. Intuitively the power at a frequency quantifies how much of $\mathbf{x}(t)$'s signal is represented by the orthogonal component, or harmonic term, $c_j e^{i\lambda_j t}$, over the time window of length T. This calculation yields the vector of powers for given frequencies, $X_k(t) = (|c_1|^2, |c_2|^2, \cdots, |c_n|^2)$, for each of the M time series which generates a multivariate time series. Interpretively, power and variance are equivalent by Parseval's theorem [9, 3] which shows that the total power in frequency space is equal to the variance in state space, or: $\sigma(\mathbf{x}_k(T)) = P(\mathbf{x}_k(T)) = \frac{1}{T}\sum_{t=1}^{T} x_k^2(t) = \sum_{j=-n}^{n} |c_j|^2$.

Empirical orthogonal functional analysis Consider a matrix of time series, $\mathbf{X}(T_k)$, where the columns index the time points, and the rows index the variables (e.g., the frequencies); this matrix is populated by $|c_j|^2$'s. Assume we have de-trended $\mathbf{X}(T_k)$ such that it is mean zero. Associated with $\mathbf{X}(T_k)$ is its covariance matrix, $\Sigma(T_k)$. By construction Σ is Hermitian so the eigenvalues are non-negative and there will always exist an orthogonal basis (i.e., a set of orthogonal eigenvectors). We can decompose $\mathbf{X}(T_k)$ into orthogonal directions of maximum variance which is equivalent to (cf. section 13.1 in [7]) decomposing $\mathbf{X}(T_k)$ into eigenvectors corresponding to the eigenvectors of $\Sigma(T_k)$ in descending order. Specifically, decompose $\mathbf{X}(T_k)$ according to $\mathbf{X}(T_k) = U\Lambda V^T$ where Λ is a diagonal matrix whose eigenvalues, σ_i, represent the contribution of variance in a given orthonormal direction in $\mathbf{X}(T_k)$. The orthogonal directions of variance, or the EOFs, are then represented by the U_i's, which are the ranked eigenvectors of covariance matrix $\Sigma(T_k) = \mathbf{X}(T_k)\mathbf{X}^T(T_k) = U\Lambda U^T$. The first EOF is the *pattern* representing the maximum variance within $\mathbf{X}(T_k)$; or, more mathematically, the first EOF is the eigenvector that minimizes $E(\|\mathbf{X} - \langle \mathbf{X}, \mathbf{e}\rangle \mathbf{e}\|^2)$. Note, $\mathbf{X}(T_k)$ must be at least a full rank matrix which in practice means that $k \geq n$.

We visualize the variation in $\mathbf{X}(T_k)$ by plotting the individual EOF vectors, the $U_i(T_k)$'s, versus time, thus creating a multivariate time series of length M. Moreover, we also estimate and plot the time-dependent fraction of energy or variance represented by the given EOF being plotted. Recall that the total power (variance), is the sum of the eigenvalues (the trace) of $\Sigma(T_k)$, or $\sigma(\mathbf{X}(T_k)) = \sum_{j=1}^{n} \lambda_j$. Using this, the fraction of the variance that EOF j represents is $\frac{\lambda_j}{\sigma(\mathbf{X}(T_k))}$.

In many situations, only the first or second EOF are of use; however, in our application the variables, power per frequency, are often highly stratified. Meaning, often but not always, the different EOFs represent the variation in power of different frequencies. Because of this, it can be useful to observe some EOFs with low fractional variance if they represent frequency bands of interest.

Explicit details of the PS and EOF computations The explicit algorithm we used in this paper follows four steps: *(i)* collect a time series of PS data, which is estimated by the machinery used to collect EEG data; *(ii)* determine a suitable EOF window size, noting that $k \geq n$, thus creating the $\mathbf{X}(T_j)$'s; *(iii)* estimate the EOF on *non-overlapping* time windows of the PS data, the $\mathbf{X}(T_j)$'s; and *(iv)* plot one or more EOFs, a n-dimensional vector, in time (cf. Figs. 2 and 4).

Interpretation of the EOFs of the time series of PS of a time series Moving back into the context where $\mathbf{X}(T_k)$ is a matrix of time series of power per frequency, the interpretation of PS, the first EOF, and the first EOF of the PS are as follows.

Power spectrum of the time series: a time series can be decomposed and represented as energy or power (if integrated over time) of the frequencies that compose the time series. Or, written differently, the time series can be rewritten in terms of power (variance) per orthogonal basis element. In this situation, the basis elements are *not chosen to maximize any quantity*, but rather as the frequencies present in the data. Moreover, while the Fourier modes are orthogonal by definition, the power per frequency, represented by

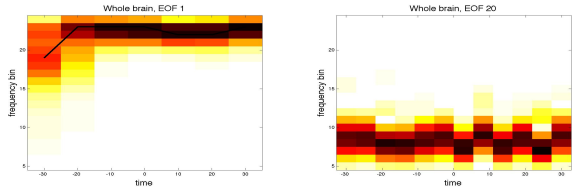

Figure 2: The 1^{st} and 20^{th} EOFs versus time before and after seizure for power spectra of an EEG time series.

the components of the $\mathbf{X}(T_k)$ matrix, are not orthogonal.

First EOF of a multivariate time series: the orthogonal direction that represents the direction of greatest (or maximized) energy or variance and can include portions of different frequencies (e.g., 3 Hz accounts for 20% , 5 Hz accounts for 40%, etc.); the first EOF is a vector that specifies what proportions of which frequencies make up the orthogonal vector in the direction of the maximum energy or variance.

First EOF of the PS of a time series: the ranked (or ordered) proportional selection of frequencies that contribute the most energy without overlapping (i.e., along the orthogonal component that captures or represents the maximum amount of energy). This is equivalent to identifying the frequencies, by proportion, that contribute the most to variance, or energy in the EEG signal. Because variance and energy are synonymous, the first EOF of the PS of a time series reveals the frequencies within the EGG signal that are the most active, important, present, or energetic.

4. Results

Identifying high resolution EOF features before and after manually identified seizure events. To study the nature of depth seizures in SAH patients, we applied EOF analysis to the PS of the EEG for $n = 20$ ranging from 1 to 20 Hz recorded at 5 second intervals ($T = 5min, k = 60$) 30 minutes before and after seizure ($M = 60min$) for several single patient with a SAH. The seizure onsets were manually identified by a neurointensivist. The signal via EOF of the PS of the EEG revealed that at the onset of seizure, the period of oscillation in frequencies changes. In the specific patient shown in Fig. 2 at seizure onset a slow oscillation appears in the first EOF representing the high frequencies; in the twentieth EOF the oscillation in frequency *changes* period from 25 to 12 minutes. This implies that as the during the seizure, the set of excited frequencies is severely constrained and highly organized. It is hoped that temporal signatures such as these can be generalized to better understand seizure, and to phenotype different types of seizure in SAH patients.

Seizure visualization and detection prior to manual seizure identification. A subset of the SAH patients we study have a depth electrode inserted in their brain to monitor electrical activity for clinical reasons and of these patients 18 of 48 displayed a "depth seizure," or a seizure that was not easily identifiable from the surface EEG. The PS of the EEG was recorded once a minute with an $n = 40$ spit into half a Hz intervals ranging from 1-20 Hz for the entire length of the patient stay. Here we set $T = 40$ minutes ($n = k = 40$).

In our example there are two features of the patient's time course we want to focus on.*First*, in the *first quarter* of the time course, the patient had a focal NCSz event detected with a depth electrode in the patients left hemisphere; this event was relatively continuous. *Second*, for the remainder of the time course the patient oscillated between no ictal (in other words no seizure or other ictal activity state) and ictal-interictal (a state in between seizures and no seizures). Both states were events predominantly deep in the brain and only observable using the EEG collected by the depth probe which was inserted in the right frontal lobe. Figure 3 shows the PS of the surface EEG. In these plots, only the strong initial seizure event is evident. In contrast, the EOF of the PS signals, Fig. 4, reveals the persistent depth seizure in the left brain only; neither the whole brain nor the right brain have a single strong enough to identify a seizure-like event in the EOF signal. This corroborates what we expect in half of the depth seizure cases — a localized seizure event that is not propagating through the rest of the brain. Therefore, in this example, applying the EOF to the PS of the surface EEG can help identify depth seizure events using *surface EEG data* that are only identifiable manually using the depth EEG and are manually unidentifiable using the PS of either the depth or the surface EEG alone.

Seizure identification in a small population of SAH patients with and without seizure. A first step toward using an EOF signal to define a seizure phenotype is to determine whether an EOF signal can be used to identify seizure by humans at a broad level. Using a data set consisting of 26 patients, 1 with a surface and 12 with depth seizures, we compared EOF visualization to PS visualization in correctly identifying seizures according to a gold standard generated by a trained neuroscientist. Accuracy was 88% for EOF versus 48% for PS, and the difference was statistically significantly different by McNemar's test ($p = 0.008$) [5]. Similarly, using the EOF of the PS there is a strong, statistically significant *linear* correlation ($\rho = 0.76$, $p = 10^{-5}$) between EOF-identified seizure and the gold standard. There was no linear correlation between the PS identified seizure and the gold standard. Relative to the data set here, the EOF was not useful for differentiating depth versus surface seizure; this lack of effectiveness is likely due to sample size (correlation for depth identification was strong but not statistically significant).

5. Discussion

EOF analysis of the PS of EEG highlights the characteristics of EEG that define seizure in SAH patients. More-

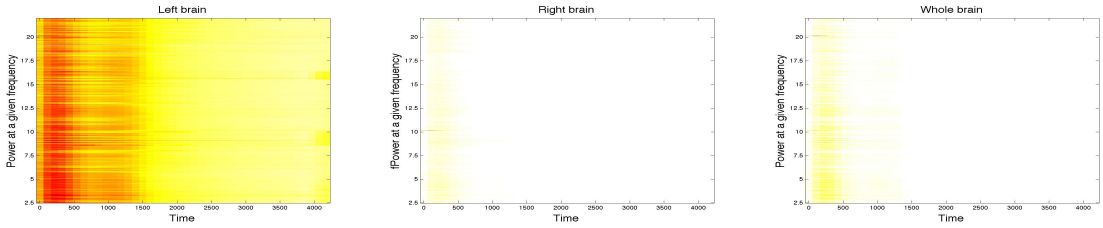

Figure 3: PS of the EEG for the left, right, and whole brain (left to right) respectively. The Note that the persistent depth seizure in the left hemisphere is not evident.

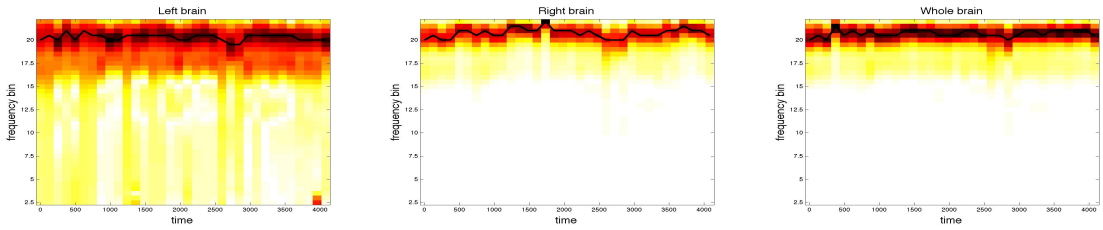

Figure 4: EOF of the PS of the EEG for the left, right, and whole brain (left to right) respectively; note depth seizure event is only apparent in the EOF of the *left* side of the brain.

over, the EOF of the PS of the EEG makes manual identification of seizure significantly easier and more reliable. As is often the case, multiple levels of data analysis, e.g., estimating the EOF of the PS of the EEG, can be very useful for revealing the important temporal content.

Given the likelihood that seizures in SAH patients have different implications for different populations of patients (e.g., older patients, patients with greater injury, etc.), discovering and quantifying the differentiating temporal signatures and tying them to outcomes will be of critical significance for both understanding and treating seizure in patients with SAH. Nevertheless scientifically controlled collection of EEG data for SAH patients are rare if nonexistent. Here we show that it is possible to use physiologic data collected for clinical reasons to better understand SAH-based pathophysiology, even though the data are collected outside of a scientifically controlled environment and contain noise, missing values, clinical intervention effects, and nonstationary trends. Nevertheless, much work remains both to automate seizure detection in SAH patients using the EOF of the PS, and to statistically define the temporal signatures that can be used to differentiate patient health and predict patient outcome.

Acknowledgments

DJA and GH were funded a grant from the National Library of Medicine, R01 LM006910. JC was funded by a grant from the NCRR-NIH, L1 RR024156. MS was funded by C.S. Draper Laboratory, Inc. grant number $SC001-0000000642$. We'd like to thank Professor Sato for discussions and the invitation, and NOLTA for hosting the conference.

References

[1] J Claassen, A Perotte, DJ Albers, S Kleinberg, JM Schmidt, B Tu, H Lantigua, LJ Hirsch, SA Mayer, ES Connolly, and George Hripscak. Electrographic seizures after subarchnoid hemorrage and derangements of brain homeostasis in humans. *Annals of Neurology*, in press 2013.

[2] P. Dayan and L. F. Abbott. *Theoretical Neuroscience*. MIT Press, 2005.

[3] LH Koopmans. *The spectral analysis of time series*. Academic press, 1974.

[4] P Lejeune-Dirichlet. On the convergence of trigonometric series which serve to represent an arbitrary function between two given limits. *Journal fur die reine und angewandte Mathematik*, 4:157–169, 1829.

[5] Q McNemar. Note on the sampling error of the difference between correlated proportions or percentages. *Psychometrika*, 12(2):153–157, 1947.

[6] P. P. Mitra and H. Bokil. *Observed brain dynamics*. Oxford University Press, 2008.

[7] H von Storch and F Zwiers. *Statistical analysis in climate research*. Cambridge Univesity Press, 1999.

[8] A. S. Weigend and N. A. Gershenfeld, editors. *Time series prediction: Forecasthing the future and understanding the past*. Addison Westley, 1994.

[9] Richard L. Wheeden and Antoni Zygmund. *Measure and integral*, volume 43 of *Monographs and textbooks in pure and applied mathematics*. Marcel Dekker, Inc., 1977.